Erschienen in: Europhysics Letters (EPL) ; 79 (2007), 3. - 30002
https://dx.doi.org/10.1209/0295-5075/79/30002

Distribution of entropy production for a colloidal particle in a nonequilibrium steady state

T. Speck[1], V. Blickle[2], C. Bechinger[2] and U. Seifert[1]

[1] *II. Institut für Theoretische Physik, Universität Stuttgart - Pfaffenwaldring 57, 70550 Stuttgart, Germany*
[2] *2. Physikalisches Institut, Universität Stuttgart - Pfaffenwaldring 57, 70550 Stuttgart, Germany*

PACS 05.40.-a – Fluctuation phenomena, random processes, noise, and Brownian motion
PACS 82.70.Dd – Colloids

Abstract – For a colloidal particle driven by a constant force across a periodic potential, we investigate the distribution of entropy production both experimentally and theoretically. For short trajectories, the fluctuation theorem holds experimentally. The mean entropy production rate shows two regimes as a function of the applied force. Theoretically, both mean and variance of the pronounced non-Gaussian distribution can be obtained from a differential equation in good agreement with the experimental data.

Nonequilibrium steady states constitute arguably the simplest class of nonequilibrium systems. They are characterized by a stationary distribution but differ crucially from equilibrium states since detailed balance is broken. As a consequence, entropy is produced at an on average positive rate. Fluctuations of the entropy production towards negative values do occur but they are severely constrained by the fluctuation theorem. This universal relation was first observed in the simulations of a sheared fluid [1] and later proven both for chaotic dynamic systems [2] and for stochastic dynamics [3,4]. In principle, the fluctuation theorem is an asymptotic statement in the long time limit. If, however, entropy is assigned to the driven system as well and not only to the coupled heat bath, the fluctuation theorem holds strictly for finite times [5]. Closely related to the fluctuation theorem are the Jarzynski [6] and Crooks [7] nonequilibrium work relations, which proved to be useful in the determination of equilibrium free energy differences in single-molecule experiments [8,9].

The fluctuation theorem constrains the probability of negative-entropy production. It does, however, not predict the distribution for positive production which is, of course, a nonuniversal function. For a better understanding of nonequilibrium steady states [10], detailed studies of the entropy production in specific systems are important. Entropy production has been studied both experimentally and theoretically for a variety of systems including Brownian particles [11], turbulent flows [12], granular systems [13], liquid crystals [14], and the ideal gas [15], mostly addressing the entropy production in the medium only. Entropy production including that of the system has been experimentally measured in an athermal two-level system [16] for which later numerical calculations of its probability distribution have been performed [17]. In the latter system, medium entropy is somewhat artifically defined and should not be associated with dissipated heat.

Colloidal particles driven by time-dependent laser traps have developed into an ideal system for quantitatively studying these new concepts in nonequilibrium statistical mechanics for essentially two reasons. First, individual trajectories can be traced and recorded in real space in comparison to ensemble averages typically obtained in scattering experiments. Second, even though the particle in a distinct nonequilibrium steady state can be driven beyond linear response, the surrounding fluid still faithfully behaves like an equilibrium thermal bath. In this letter, we exploit these features to analyze entropy production in a nonequilibrium steady state consisting of a single particle driven by a constant force across a periodic potential [18]. In contrast to previous experiments on colloids in time-dependent harmonic potentials [19,20] such a periodic potential in general leads to non-Gaussian distributions for quantities like applied work, dissipated heat and generated entropy [21]. In fact, we will show that even the mean entropy production rate shows a pronounced crossover as a function of the applied force. An additional advantage of such a colloidal system compared to driven bulk systems is that once the potential is known,

the experimental data can be compared to independent numerical calculations.

We study a single colloidal particle in a toroidal geometry driven into a nonequilibrium steady state. The overdamped motion of the colloidal particle is governed by the Langevin equation

$$\dot{x}(t) = \mu_0 \left(-\frac{\partial V}{\partial x} + f \right) + \zeta(t) \equiv \mu_0 F(x) + \zeta(t) \qquad (1)$$

with a periodic potential $V(x+L) = V(x)$ and periodicity L. The thermal noise ζ describes the coupling of the particle to the surrounding fluid modeling the heat bath with temperature T. The noise has zero mean and correlations $\langle \zeta(t)\zeta(\tau)\rangle = 2D_0\delta(t-\tau)$. The correlation strength D_0 of the heat bath is connected with the bare mobility of the particle μ_0 by the Einstein relation $D_0 = k_\mathrm{B}T\mu_0$. The crucial assumption is that we require the heat bath to be and to stay in equilibrium at the constant temperature T. We can then identify the dissipated heat q as the change of entropy

$$\Delta s_\mathrm{m}[x(\tau)] = \int \frac{\mathrm{d}q}{T} = \frac{1}{T}\int_0^t \mathrm{d}\tau\, \dot{x}(\tau) F(x(\tau)) \qquad (2)$$

in the heat bath or medium along a single trajectory $x(\tau)$ of length t [5,22]. Beside this entropy production in the medium, we can assign an entropy to the system itself even in nonequilibrium [5] by defining

$$s(\tau) \equiv -k_\mathrm{B} \ln p_\mathrm{s}(x(\tau)). \qquad (3)$$

Here, the measured or calculated stationary distribution $p_s(x)$ of the position in the steady state is evaluated along the specific trajectory $x(\tau)$. Then the total entropy production $\Delta s_\mathrm{tot} = \Delta s_\mathrm{m} + \Delta s$ fulfills the fluctuation theorem

$$\frac{P(-\Delta s_\mathrm{tot})}{P(+\Delta s_\mathrm{tot})} = e^{-\Delta s_\mathrm{tot}/k_\mathrm{B}} \qquad (4)$$

for any trajectory length t, where $P(-\Delta s_\mathrm{tot})$ is the probability of entropy annihilating trajectories which is compared to those generating the same positive amount of entropy.

The physical source of entropy production in our setup is the nonconservative force f which breaks detailed balance and leads to a permanent dissipation of heat into the surrounding heat bath. Breaking of detailed balance is quantified by the mean local velocity $v_\mathrm{s}(x)$, *i.e.*, the velocity averaged over the subset of trajectories passing x. With the stationary current j_s and probability $p_\mathrm{s}(x)$, the mean local velocity can be expressed as $v_\mathrm{s}(x) = j_\mathrm{s}/p_\mathrm{s}(x)$. Introducing an effective potential $\phi(x) \equiv -\ln p_\mathrm{s}(x)$, the total force

$$\mu_0 F(x) = v_\mathrm{s}(x) - D_0 \frac{\partial \phi(x)}{\partial x} \qquad (5)$$

splits into the local mean velocity and the gradient of the effective potential [23]. From the definition of the entropy (3) it is clear that the change of the effective potential along a stochastic trajectory equals the change in system entropy

$$\Delta s = k_\mathrm{B}\Delta\phi \equiv k_\mathrm{B}[\phi(x_t) - \phi(x_0)], \qquad (6)$$

where x_0 and x_t are the initial and final position of the particle, respectively.

The change in medium entropy depends only on the initial and final position of the particle, since in our case, due to stationarity, eq. (2) simplifies to

$$T\Delta s_\mathrm{m}(x_0, x_t) = -\Delta V + f\Delta x. \qquad (7)$$

Beside the sum of system and medium entropy, we can obtain an independent expression for the total entropy production by inserting the force (5) into eq. (2). We then get after one integration by parts and cancellation of the boundary term

$$\Delta s_\mathrm{tot}[x(\tau)] = \frac{k_\mathrm{B}}{D_0}\int_0^t \mathrm{d}\tau\, \dot{x}(\tau) v_\mathrm{s}(x(\tau)), \qquad (8)$$

which depends on the whole trajectory $x(\tau)$.

We generate a nonequilibrium steady state experimentally by driving a single silica bead with diameter 1.85 μm along a toroidal trap with radius $R_0 \simeq 2.2\,\mu$m implying a periodicity of $L = 2\pi R_0$. The trap is created by tightly focused optical tweezers rotating with a frequency of $\nu_\mathrm{T} \simeq 510\,\mathrm{Hz}$ [24]. At this frequency, the particle experiences a periodic driving force whenever it is "kicked" by the passing laser beam but the particle cannot follow the beam directly. Since video microscopy is not able to resolve these single kicking events (due to its spatial (50 nm) and temporal (50 ms) resolution), the particle is effectively subjected to a constant force f, thus driving it into a nonequilibrium steady state [25]. An additional periodic potential $V(x)$ (see fig. 1) with depth V_0 is created by modulating the intensity of the optical tweezers with an electro-optical modulator (EOM) whose input is synchronized with the tweezers' scanning motion. The potential $V(x)$ and the driving force

$$f = \frac{1}{\mu_0 L}\int_0^L \mathrm{d}x\, v_\mathrm{s}(x) \qquad (9)$$

are reconstructed from the measured distribution $p_\mathrm{s}(x)$ and current j_s [26].

The position of the particle in polar coordinates is sampled with frequency 20 Hz. The deviation of the radial component $\delta r \simeq 0.06\,\mu$m with $\delta r/R_0 < 3\%$ is small enough to justify the assumption of an effectively one-dimensional motion. We record one long trajectory from which we determine the stationary probability $p_\mathrm{s}(\alpha)$ of the angular position α shown in fig. 1. The trajectory is then divided in overlapping segments of N points such that the angles α_i with $1 \leqslant i \leqslant N$ form discrete trajectories. The total entropy production along one discrete trajectory is calculated from eq. (8) as

$$\Delta s_\mathrm{tot}^{(N)} = k_\mathrm{B}\frac{j_\mathrm{s}R_0^2}{D_0}\sum_{i=2}^{N-1}\frac{\alpha_{i+1} - \alpha_{i-1}}{2p_\mathrm{s}(\alpha_i)}. \qquad (10)$$

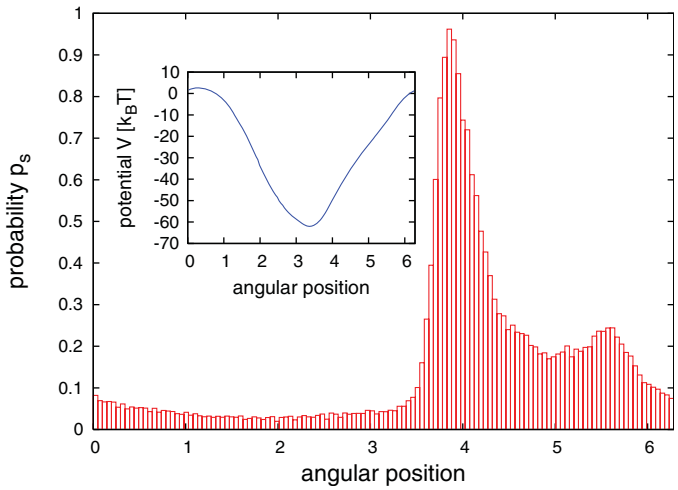

Fig. 1: Stationary probability distribution $p_s(x)$ for a cosine input signal to the EOM with driving force $f = 14.2 k_B T/\mu$m. The inset shows the reconstructed actual potential $V(x)$ with $V_0 = 65.6 k_B T$.

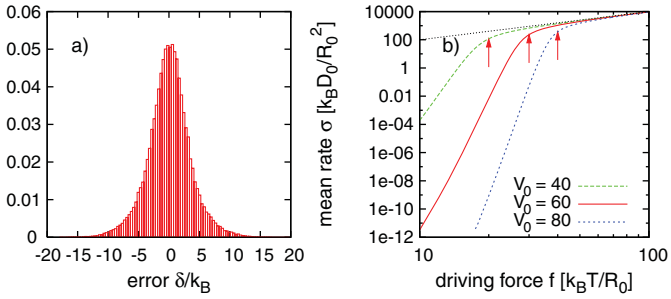

Fig. 2: a) The difference $\delta \equiv \Delta s_{\rm tot}^{(N)} - \Delta s_{\rm m} - \Delta s$ after $t = 5$ s between the total entropy production (10) determined from a discretely measured trajectory and the sum of medium (7) and system entropy (6) for parameters $V_0 = 80.4 k_B T$ and $f = 16.4 k_B T/\mu$m. b) Mean entropy production rate σ determined numerically for a potential $V(x) = (V_0/2)\cos x$ *vs.* driving force f. The dotted line indicates the limiting behavior $\sigma \approx f^2$ for large forces and the arrows mark the critical forces $f_c = V_0/(2R_0)$.

In fig. 2(a), the deviation $\delta \equiv \Delta s_{\rm tot}^{(N)} - \Delta s_{\rm m} - \Delta s$ of the total entropy production (10) from the independently measured medium entropy production (7) and the entropy production of the system itself (6) is shown. This deviation is a Gaussian centered around zero with a standard deviation of $3.5 k_B$, which corresponds to a relative error $< 3\%$ given the mean $\langle \Delta s_{\rm tot} \rangle \simeq 121.3 k_B$. This small error shows that the discretization of the stochastic velocity $\dot{x}$ within the integral eq. (8) is a very good approximation even for a time resolution of 50 ms. This is not obvious *a priori* due to the mathematically nondifferentiable stochastic paths $x(\tau)$.

In fig. 3, the data are plotted in the form of the fluctuation theorem (4) for different trajectory lengths t. The fluctuation theorem can only be tested directly in

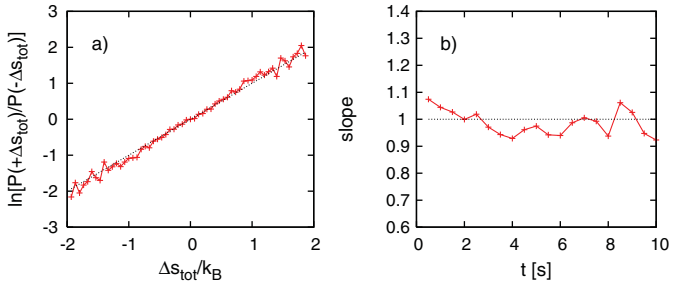

Fig. 3: a) Test of the fluctuation theorem (4) for $t = 0.75$ s, where the logarithm $\ln[P(+\Delta s_{\rm tot})/P(-\Delta s_{\rm tot})]$ is plotted *vs.* $\Delta s_{\rm tot}$. The dashed line indicates the expected slope of one and in b) the effective slope is plotted with increasing trajectory lengths. (Parameters: $V_0 = 65.6 k_B T$, $f = 14.2 k_B T/\mu$m.)

a small window of the histogram centered around zero due to the need for negative events. Since the distribution $P(\Delta s_{\rm tot})$ shifts towards larger values with increasing time, negative values of $\Delta s_{\rm tot}$ become less probable and the statistics is good enough only for relatively small times.

The driving force f tilts the potential $V(x)$ and lowers the potential barrier which at the critical force f_c vanishes and deterministic running solutions start to exist. For a cosine potential, the critical force turns out to be $f_c = V_0/(2R_0)$. In fig. 2(b), the mean entropy production rate

$$\sigma \equiv \langle \partial_t \Delta s_{\rm tot} \rangle = \frac{k_B}{D_0} \langle v_s^2 \rangle = \frac{k_B}{D_0} j_s^2 R_0^2 \int_0^{2\pi} {\rm d}\alpha \, p_s^{-1}(\alpha) \quad (11)$$

is plotted *vs.* the driving force for three potential depths V_0. The two limiting cases

$$\sigma \approx \begin{cases} (\mu_0/T) f^2 & (f \gg f_c), \\ (\Delta w/T) r_K & (f \ll f_c) \end{cases} \quad (12)$$

are understood easily. For large forces $f \gg f_c$, the potential becomes irrelevant and the particle diffuses freely with drift velocity $\propto f$. The mean entropy production rate in this case becomes $(\mu_0/T) f^2$. For small forces $f \ll f_c$, the particle is mostly trapped within one minimum from which it escapes with the Kramers' rate $r_K = r_0 \exp\{(-V_0 + fL/2)/k_B T\}$, where r_0 is the attempt rate [27]. If the particle moves to the next minimum, the driving force has spent the work $\Delta w = fL$.

This crossover can also be observed in the histograms of $\Delta s_{\rm tot}$. In fig. 4(a), the case with the critical force $f \simeq f_c$ is plotted. The work spent by the driving force is the product of force times the displacement of the particle such that trajectories corresponding to n revolutions of the particle lead to an entropy production peaked at the dashed vertical lines with $\Delta s_{\rm tot} = n \Delta w/T$. In fig. 4(b), the potential depth V_0 has been decreased at the same driving force, leading to $f > f_c$. In this case the distribution of $\Delta s_{\rm tot}$ starts to "run", *i.e.*, the peak positions are not fixed anymore at the vertical lines. However, this is where they still reach their maximum as demonstrated by the rightmost histogram for $t = 21.5$ s.

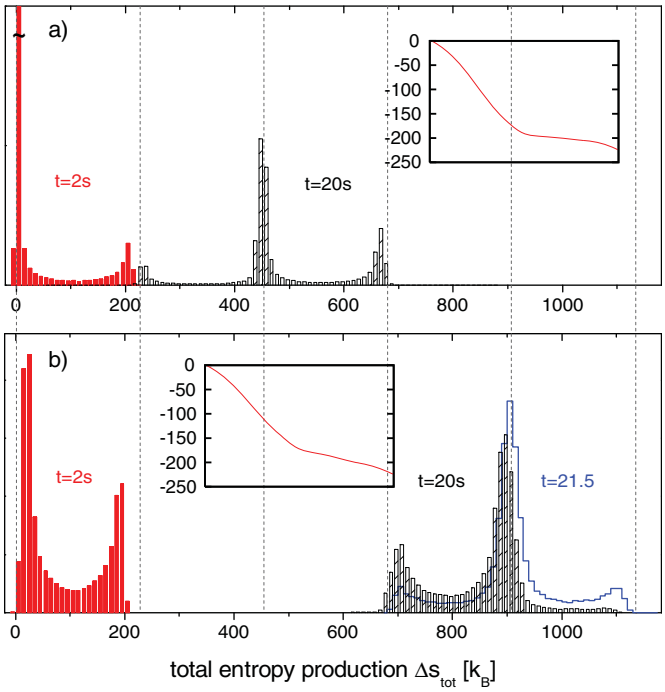

Fig. 4: Histograms of total entropy production $\Delta s_{\rm tot}$ at the crossover from locked to running state: a) $V_0 = 80.4 k_{\rm B}T$ and $f = 16.4 k_{\rm B}T/\mu$m which corresponds to the critical force, b) $V_0 = 61.7 k_{\rm B}T$ and the same force $f = 16.4 k_{\rm B}T/\mu$m corresponding to the running state. In both graphs, the left histograms (closed bars) are recorded for trajectories of length $t = 2$ s, the right histograms (hatched bars) for $t = 20$ s. In addition, b) shows as a solid line for $t = 21.5$ s an almost symmetric histogram (with respect to its peak). The dashed vertical lines are separated by the amount of work $\Delta w = fL$ spent by the driving force f in one revolution. The insets display the tilted potentials $V(x) - fx$ for the two cases.

The probability distribution $P(\Delta s_{\rm tot})$ of the total entropy production is a nonuniversal function distinctly non-Gaussian and evolving in time. In order to compare the experimental data to theory, we need to calculate $P(\Delta s_{\rm tot})$ independently. In ref. [28] an equation governing the time evolution of the joint probability distribution $\rho(x, r = \Delta s_{\rm tot}, t)$ was derived[1]. The conditional moments $m_n(x,t) \equiv \int {\rm d}r\, r^n \rho(x,r,t)$ are the contribution of all trajectories ending in x at time t to the moments

$$M_n(t) \equiv \langle (\Delta s_{\rm tot})^n \rangle = \int_0^L {\rm d}x\, m_n(x,t) \qquad (13)$$

of $P(\Delta s_{\rm tot})$. Following ref. [28], the time evolution of the conditional moments reads

$$\frac{\partial m_n(x,t)}{\partial t} = \hat{L} m_n(x,t) + S_n(x,t), \qquad (14)$$

[1]Equation (22) in ref. [28] was derived originally for the so called "housekeeping heat" $Q_{\rm hk}$. Since in our case $\Delta s_{\rm tot} = Q_{\rm hk}/T$, this equation holds also for the total entropy production.

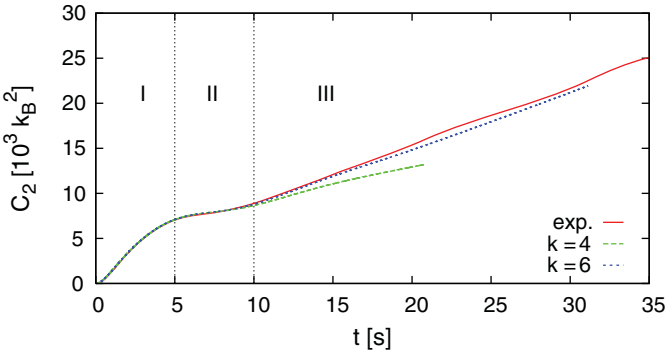

Fig. 5: Comparison of the variance $C_2(t)$ between experimental data and the solution of eq. (14). The experimental data has been obtained from 120.000 trajectories for $V_0 = 65.6 k_{\rm B}T$ and $f = 14.2 k_{\rm B}T/\mu$m. k is the number of Fourier coefficients used for parameterizing the actual potential $V(x)$, see the inset of fig. 1. The three regimes I, II, and III are discussed in the main text.

where $\hat{L} \equiv -\partial_x \left[\mu_0 F(x) - D_0 \partial_x\right]$ is the Fokker-Planck operator determining the Brownian motion of the particle. The source term

$$S_n = -n k_{\rm B} \left[2 \frac{\partial}{\partial x} v_{\rm s} - \frac{v_{\rm s}^2}{D_0}\right] m_{n-1} + n(n-1) k_{\rm B}^2 \frac{v_{\rm s}^2}{D_0} m_{n-2}$$

couples the evolution of the n-th conditional moment m_n to conditional moments of lower order where $m_0(x) = p_{\rm s}(x)$ is the stationary solution of $\hat{L} m_0 = 0$.

For the numerical calculation, we use the experimentally obtained potential $V(x)$, driving force f, stationary current $j_{\rm s}$, and probability distribution $p_{\rm s}(x)$ for the run shown in fig. 1 measured in the vicinity of the critical force $f \simeq f_{\rm c}$. Because of the periodicity of $m_0(x+L) = m_0(x)$, $m_n(x)$ as well as the source terms $S_n(x)$ are also periodic for $n \geqslant 0$. Equation (14) is therefore easily solved numerically in Fourier space which we have done for the first two moments $M_{1,2}$. From these i) the mean M_1 and ii) the variance $C_2 \equiv M_2 - M_1^2$ are obtained. The mean $M_1(t) = \sigma t$ is a straight line from which we can extract σ. First, we fit the experimental data with $\sigma \simeq 17.15 k_{\rm B}$/s. Second, we fit the numerical solution (13) leading to $\sigma \simeq 17.12 k_{\rm B}$/s in excellent agreement with the experimental data. The latter value of σ is also obtained from eq. (11) which only involves the measured distribution $p_{\rm s}(x)$ and current $j_{\rm s}$.

In fig. 5, we plot the variance C_2 together with its experimental counterpart. The time-dependence of the variance $C_2(t)$ resembles roughly that of the mean square displacement. During the first regime (I) in fig. 5, the particle explores its vicinity until it reaches on average the potential barrier. While surmounting the barrier (II), the spreading of the distribution slows down and then again increases approximately linearly (III). Analyzing the data at the critical force $f \simeq f_{\rm c}$ demonstrates the sensitivity of the entropy production. The slope in regime III is especially sensitive with respect to both the potential

and the driving force. Therefore the force f used in the numerical calculations has been fitted with value $f \simeq 13.9\, k_{\mathrm{B}}T/\mu\mathrm{m}$ to match the experimentally determined $C_2(t)$. This corresponds to a deviation of about 2% compared to the value $f \simeq 14.2\, k_{\mathrm{B}}T/\mu\mathrm{m}$ calculated from eq. (9), which is well within the estimated error of the force. The accuracy of the potential's parameterization is controlled by the number k of Fourier coefficients used leading to a better agreement with higher value for k. Despite the good agreement for the mean and variance, the numerical calculation of higher cumulants shows an increasing sensitivity with respect to the accuracy of the measured quantities needed as input.

In summary, we have measured experimentally the distribution of the total entropy production caused by driving a colloidal particle in a toroidal geometry. The system exhibits a transition from exponentially small to quadratic mean entropy production rate depending on the ratio fL/V_0 between driving force f and potential depth V_0, which can be seen in the histograms of the entropy production as well. The time evolution of the moments of the total entropy production is described by a differential equation. The procedure outlined above becomes less reliable for higher cumulants due to accumulating errors with increasing trajectory length. For long trajectories, direct calculation of the asymptotic large deviation function of the entropy production rate seems preferable. Its extraction from experimental data, however, might pose a challenge.

REFERENCES

[1] Evans D. J., Cohen E. G. D. and Morriss G. P., *Phys. Rev. Lett.*, **71** (1993) 2401.
[2] Gallavotti G. and Cohen E. G. D., *Phys. Rev. Lett.*, **74** (1995) 2694.
[3] Kurchan J., *J. Phys. A: Math. Gen.*, **31** (1998) 3719.
[4] Lebowitz J. L. and Spohn H., *J. Stat. Phys.*, **95** (1999) 333.
[5] Seifert U., *Phys. Rev. Lett.*, **95** (2005) 040602.
[6] Jarzynski C., *Phys. Rev. Lett.*, **78** (1997) 2690.
[7] Crooks G. E., *Phys. Rev. E*, **60** (1999) 2721.
[8] Collin D., Ritort F., Jarzynski C., Smith S. B., Tinoco I. and Bustamante C., *Nature*, **437** (2005) 231.
[9] Ritort F., *J. Phys.: Condens. Matter*, **18** (2006) R531.
[10] Zia R. and Schmittmann B., *J. Phys. A: Math. Gen.*, **39** (2006) L407.
[11] Andrieux D., Gaspard P., Ciliberto S., Garnier N., Joubaud S. and Petrosyan A., *Phys. Rev. Lett.*, **98** (2007) 150601.
[12] Ciliberto S., Garnier N., Hernandez S., Lacpatia C., Pinton J.-F. and Ruiz Chavarria G., *Physica A*, **340** (2004) 240.
[13] Feitosa K. and Menon N., *Phys. Rev. Lett.*, **92** (2004) 164301.
[14] Goldburg W. I., Goldschmidt Y. Y. and Kellay H., *Phys. Rev. Lett.*, **87** (2001) 245502.
[15] Cleuren B., Van den Broeck C. and Kawai R., *Phys. Rev. E*, **74** (2006) 021117.
[16] Tietz C., Schuler S., Speck T., Seifert U. and Wrachtrup J., *Phys. Rev. Lett.*, **97** (2006) 050602.
[17] Imparato A. and Peliti L., *J. Stat. Mech.: Theor. Exp.* L02001 (2007).
[18] Risken H., *The Fokker-Planck Equation*, 2nd edition (Springer-Verlag, Berlin) 1989.
[19] Wang G. M., Sevick E. M., Mittag E., Searles D. J. and Evans D. J., *Phys. Rev. Lett.*, **89** (2002) 050601.
[20] Trepagnier E. H., Jarzynski C., Ritort F., Crooks G. E., Bustamante C. J. and Liphardt J., *Proc. Natl. Acad. Sci. U.S.A.*, **101** (2004) 15038.
[21] Gomez-Marin A. and Pagonabarraga I., *Phys. Rev. E*, **74** (2006) 061113.
[22] Blickle V., Speck T., Helden L., Seifert U. and Bechinger C., *Phys. Rev. Lett.*, **96** (2006) 070603.
[23] Speck T. and Seifert U., *Europhys. Lett.*, **74** (2006) 391.
[24] Lutz C., Reichert M., Stark H. and Bechinger C., *Europhys. Lett.*, **74** (2006) 719.
[25] Faucheux L., Stolovitzky G. and Libchaber A., *Phys. Rev. E*, **51** (1995) 5239.
[26] Blickle V., Speck T., Seifert U. and Bechinger C., *Phys. Rev. E*, **75** (2007) 060101.
[27] Hänggi P., Talkner P. and Borkovec M., *Rev. Mod. Phys.*, **62** (1990) 251.
[28] Speck T. and Seifert U., *J. Phys. A: Math. Gen.*, **38** (2005) L581.